JMEPEG
https://doi.org/10.1007/s11665-022-07005-x

1059-9495/$19.00

TECHNICAL ARTICLE

Effect of Black Phosphorus Oxidation on Tribological Properties of Polytetrafluoroethylene-Based Composites

Zheng Wang, Lina Zhu, Guoxin Xie, and Xiaoyong Ren

Submitted: 21 February 2022 / Revised: 14 March 2022 / Accepted: 11 April 2022

Black phosphorus (BP) as an emerging two-dimensional material has been found that it possesses excellent potential applications in a variety of fields. Recently, it has been also proved that BP can exhibit excellent lubricating properties when it was used as water- or oil-based lubricant additive. In the present work, in order to explore the tribological properties of BP nanoflakes used as the solid filler in polytetrafluoroethylene (PTFE), spark plasma sintering (SPS) was used to prepare the BP/PTFE composites. Meanwhile, in consideration of the characteristics of BP easy to be oxidized, BP was actively oxidized to prepare the degraded BP (d-BP)/PTFE composites. Then Si_3N_4 balls were used as counterpart balls to conduct tribological experiments. The results of tribological experiment showed d-BP/PTFE composites with a d-BP content of 5 wt.% exhibited the best tribological properties under dry sliding and water environment condition. The characterizations and analyses of the counterpart balls and worn surfaces demonstrated that a layer of transfer film composed of phosphorus oxide reduced the coefficient of friction (COF) and wear rate. Besides, when the composites were used in an environment of water, the phosphorus oxide on the surface can dissolve in water and form a hydrogen bond network and thus further reduced friction.

Keywords black phosphorus, composite, lubrication property, polytetrafluoroethylene

1. Introduction

Polytetrafluoroethylene (PTFE) is a kind of polymer material which has a chemical structure of $-[-CF_2-CF_2-]_n-$. In consideration of the high bond energy of C-F and the highly symmetrical atomic structure of F elements, PTFE showed the excellent thermal and chemical stability. In addition, PTFE also has high electrical resistivity and low coefficient of friction (COF). Owing to the excellent properties, PTFE has been widely used as artificial blood vessel material (Ref 1), flexible electronic matrix material (Ref 2), high speed bearing material (Ref 3) and self-lubricating materials (Ref 4-7) in various fields since it was developed in 1938. In particular, when it was used as self-lubricating material, PTFE exhibits low COF ($\leq$ 0.1) because of the rapid formation of a lubricating transfer film in the contact region. However, PTFE also exhibits some obvious disadvantages when it is used as the self-lubricating material. The poor mechanical properties and the tendency to form the transfer films would limit the service life of the PTFE-based component. Hence, many researches have been done to reduce the wear rate of PTFE without losing the low COF (Ref 8-13). So far, it is a common way to improve the wear resistance of PTFE by adding fillers. The commonly used fillers can be divided into particles, fibers, and two-dimensional (2D) materials according to the shape of the fillers. Normally, different kinds of fillers can provide different enhancement effects. Wang et al. added four kinds of micrometer-sized ceramic particles (SiC, Si_3N_4, SiO_2 and h-BN) into PTFE to evaluate the tribological properties of the composites. It is found that the wear rate of the composite with 20 wt.% SiO_2 particles addition could decrease about three orders of magnitude. Meanwhile, the lubricating films formed on the worn surface can steady exist for a long time, which hindered the further wear of the composites (Ref 14). High-strength fiber could also be used as additive in PTFE to improve its mechanical properties and wear resistance. However, the COF of the composites are always increased at the same time (Ref 15-17). Some other kinds of polymers also exhibit excellent self-lubricating and wear resistance properties (Ref 18-21). Polyimide (PI) is also a polymer which is well known for possessing excellent mechanical properties and chemical stability, when it was mixed with PTFE, the resulting composite can obtain outstanding tribological and mechanical properties. Mu et al. prepared PI/PTFE composite and reinforced by ZnO nanoparticle, it was found that the wear loss of the composite decreased as well as the COF, the strong interfacial interaction between additive and matrix effectively improved the mechanical properties (Ref 22). 2D materials are well known for the unique physical and chemical properties. Some 2D materials such as graphene, MoS_2 and h-BN, exhibit low COF because of the low interlayer interaction and easy sliding nature between neighboring atomic

Zheng Wang, School of Engineering and Technology, China University of Geosciences, Beijing 100083, China; **Lina Zhu**, School of Engineering and Technology, China University of Geosciences, Beijing 100083, China; and Zhengzhou Institute, China University of Geosciences, Zhengzhou 451283, China; **Guoxin Xie**, State Key Laboratory of Tribology, Department of Mechanical Engineering, Tsinghua University, Beijing 100084, China; and **Xiaoyong Ren**, School of Mechanical, Electronic & Information Engineering, China University of Mining & Technology, Beijing 100083, China. Contact e-mails: 15650702597@163.com, zhulina@cugb.edu.cn, xgx2014@tsinghua.edu.cn, xiaoyong_ren@cumtb.edu.cn.

Published online: 23 May 2022

layers. Besides, when the atomic layers of the 2D materials are sliding against other counter surfaces, they also showed low surface friction (Ref 23). Based on the excellent tribological properties, a lot of researches focused on the studies of PTFE filled with 2D materials. Wang et al. produced the PTFE composites with MoS_2 and carbon fiber (CF) addition. The CF/MoS_2/PTFE composites exhibited the high hardness and the low COF of about 0.04, which was 61% reduction as compared with that of the pure PTFE (Ref 24). Recently, black phosphorus (BP) as a new kind of 2D materials has exhibited outstanding properties in electronic, optics, thermology, biocompatibility and other fields, which have made it the potential graphene alternative (Ref 25-28). Besides, BP also exhibits excellent lubricating property. Since Wang et al. found that BP nanosheets can be used as oil-based lubricant additives and the reinforcement phase in polymer in 2018 (Ref 29), a lot of studies started to focus on the application of BP in tribology (Ref 30-32). Moreover, Peng et al. compared the tribological behavior of pure PTFE, BP-PTFE and graphite-PTFE composite films, and it was found that BP could help PTFE to form a durable film, which lead to the composite displayed a COF reduced by 61% (Ref 33). Lv et al. prepared BP/PEEK/PTFE and BP/CF/PTFE composites and then compared their tribological properties with other PTFE-based composites. The results showed that the additive of BP nanosheets can efficiently reduce the COF and wear rate (Ref 34) The studies of Peng and Lv demonstrated that BP nanosheets have a positive effect on the tribological property of PTFE-based composites. BP has the characteristic to be easily oxidized in air. In order to prevent the oxidization of BP and keep the excellent electrical properties, many experiments have been done (Ref 35, 36). However, it was found that the oxidization of BP was beneficial to reduce the friction coefficient when it was used as lubricant additives (Ref 37). It was observed that an interfacial water layer intercalated between the degraded BP flake and the SiO_2/Si substrate, resulting in the superlubricity behavior at the BP/SiO_2 interface (Ref 39). Being inspired by the above-mentioned work, a way of using degraded BP to realize low-friction was presented herein. In this work, BP/PTFE and degraded BP (d-BP)/PTFE composites were prepared to evaluate and discuss the effect of black phosphorus oxidation on macroscopic friction. In addition, the tribological behaviors of BP/PTFE and d-BP/PTFE composites in water environment was also investigated. After the friction and wear tests, a scanning electron microscopy (SEM) and an x-ray photoelectron spectroscopy (XPS) were used to characterize the worn surfaces and the tribopair surfaces to propose the possible lubrication mechanisms.

2. Experimental Details

2.1 Materials

The materials used in this study are PTFE powders (average particle size: 10μm, Jinhong Suhua), red phosphorus (RP) (AR, 98.5%) powders and H_2O_2 (30 wt.%, Aladdin). The BP nanoflakes were obtained by a method of high energy mechanical milling (HEMM) technique (Ref 30). After the ball milling, the BP powders were analyzed with x-ray diffraction (XRD; D8-Advance, Bruker) and x-ray photoelectron spectroscopy (XPS; PHI Quantera II, Ulvac-Phi Inc.).

2.2 Characterizations of BP Nanoflakes

The crystalline composition of the powder was determined by XRD. Figure 1 exhibits the XRD results of the RP powders and the BP powders obtained by HEMM, respectively. It can be seen that there is no obvious crystal diffraction peak in the curve of RP powders, which corresponded to the amorphous structure of RP, while obvious diffraction peaks were found in the curve of obtained BP powders. According to the previous report (Ref 40), the peak positions of BP indicated that the RP powders have been converted successfully to BP after the ball milling. The chemical composition was also characterized by XPS. Figure 2 shows the XPS spectrum of the P 2p peaks of the BP powders. Two peaks at 129.3 and 130.1 eV appear, corresponding to the characteristic peaks of the P-P bond in the P 2p3/2 and P 2p1/2 orbitals in the BP crystal, respectively (Ref 39). Besides, there also exists a broad peak at 134.0 eV, which is consistent with the oxidized phosphorus (P_xO_y). It is because that BP is very susceptible to oxidation in the air (Ref 38).

2.3 Preparation of Composites

The powders used for sintering were mixed as the following method: BP nanoflakes and PTFE powders were dispersed in 40 ml ethanol with an ultrasonic dispersion for 30 minutes, and then, the dispersion liquid was magnetically stirred for 1 hour to ensure the powders were dispersed completely. After stirring, the dispersion liquid was pumped and filtered to obtain the mixture powders, and the damp powders were vacuum dried at 60 °C for 5 h. In this way, we prepared BP/PTFE and degraded BP(d-BP)/PTFE composite powders with the filler mass fractions of 3, 5, 7 and 9 wt.%, respectively. It should be noted that during the preparation of the d-BP/PTFE composites, the BP powders were firstly oxidized with H_2O_2 in ethanol, and the ratio of H_2O_2 to BP powders was 0.3:1. After oxidization, PTFE powders were added into the dispersion liquid. For the sintering process, spark plasma sintering (SPS) was chosen as the sintering method, which has the ability to heat while loading. Pure PTFE and composite materials were prepared with the condition shown in Fig. 3. In this process, the applied pressure was 10 MPa, and the powders were heated to 240 °C in 20 min, then kept at the temperature for 20 min. After sintering, the samples were cooled in the furnace. When the temperature of the composite material was under 80 °C, the

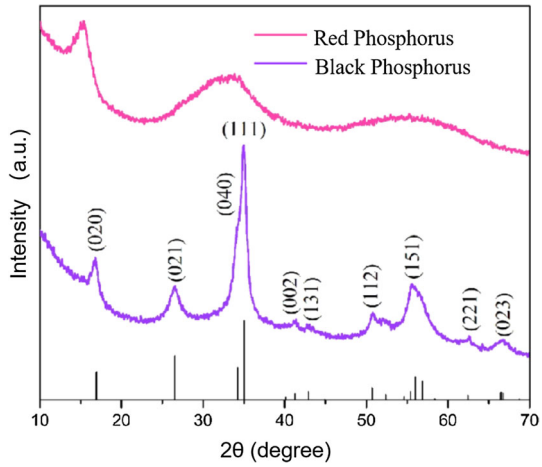

Fig. 1 The XRD results of RP and BP powders

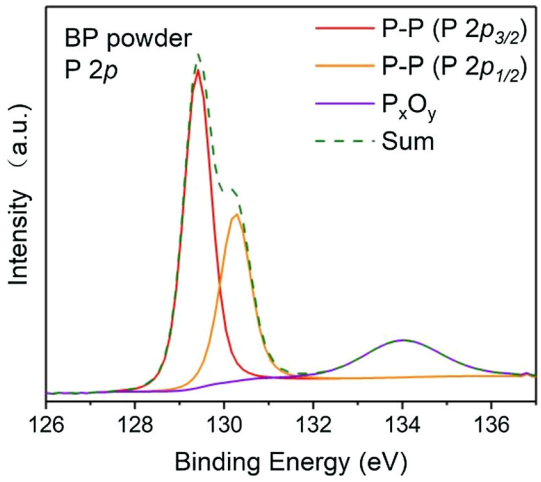

Fig. 2 X-ray photoelectron spectra of P 2p peaks of the BP powders

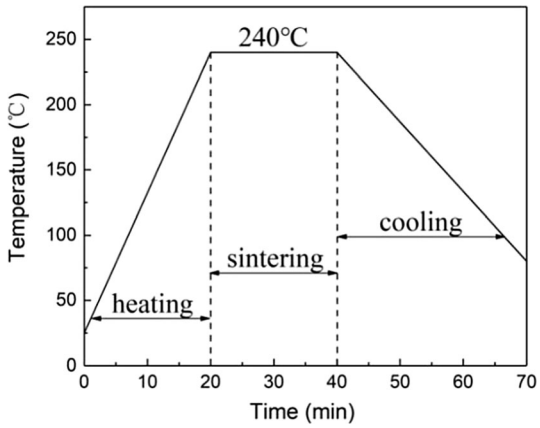

Fig. 3 Heating curve of the sinter stage

sintered samples could be taken out of the furnace. At last, the prepared composite material was polished with abrasive papers to obtain a smooth surface (abrasive paper grade: #800 ~ # 4000).

2.4 Tribological Tests

The reciprocating mode of ball-counting contact on a multifunctional friction and wear tester (UMT-3, Brucker) was used to characterize the tribological properties, with the linear sliding module as the fixture. When the water environment was needed, 30μL deionized water was introduced into the gap between the ball and composite. Silicon nitride balls with a diameter of 4 mm were used as the tribopair (Ra=0.25μm). The experimental condition was atmospheric environment, and temperature was 26 ± 2 °C, relative humidity was 40 ~ 55 RH%. Prior to the tribological experiment, the silicon nitride balls and composites were ultrasonically cleaned in ethanol for 20 min. The parameters of reciprocating sliding friction experiment are set as follows: normal load was 3 N; frequency 3 Hz (corresponding maximum pressure:76.13 MPa); vibration stroke 4 mm; experimental time 1800 s; and a new silicon nitride ball was used for each experiment. After the tribological tests, a 3D surface of white light interference profilometer (ZYGO NexView) was used to characterize the grinding crack region and measure the wear volumes, and then the wear rate (Q) of each sample was obtained by:

$$Q = \frac{V_w}{FS}$$

where V_w was wear volume (mm^3); F and S represent applied load (N) and total distance (mm), respectively (Ref 41).

2.5 Morphological Analysis of Wear Surfaces

The wear area was characterized with a HITACHI SU8220 field emission scanning electron microscope (SEM) at an operating voltage of 5 kV. The energy-dispersive spectroscopy (EDX) was used to observe the wear surfaces and the upper ball surface after tests. PHI Quantera II x-ray photoelectron spectroscopy (XPS) with monochromatic Al Kα source was also used to analyze the chemical composition of the transfer film. Finally, the possible wear mechanism of BP/PTFE and d-BP/PTFE composites was discussed.

3. Results and Discussion

3.1 Friction and Wear Properties of the Prepared Composites Under Dry Sliding Conditions

Figure 4(a) shows the variation curves in the COFs of PTFE and the composites with different BP and d-BP contents over the sliding time. It can be seen that all the curves are relatively smooth, and the PTFE exhibits the highest COF among the samples. The average COFs are shown in Fig. 4(b). All the average COF of the composites showed a decreasing trend initially and then an increasing trend with the increase of BP content or d-BP content. The lowest COFs are the samples both with a content of 5 wt.%. It is apparent that the variation of COF is nonlinear. Compared with the COF of pure PTFE (0.12), the COF of the composite with 5 wt.% BP addition (0.092) reduces about 23.3%, while the COF of the composite with 5 wt.% d-BP/PTFE has a sharp decrease (reduced about 35%, with a COF of about 0.078). The wear volumes of the composites were measured with a white light interference profilometer, and the wear rates were calculated, as summarized in Fig. 5. The wear rate of pure PTFE was about 5.345×10^{-4} $mm^3 \cdot N^{-1} \cdot m^{-1}$. Corresponding to the results of COF, the wear rate showed the same trend that decreases initially with the increase of the filler content. When the contents of BP and d-BP were about 5 wt.%, the wear rates reached the lowest values. The wear rate started to increase with the further increase of the filler content. The pure PTFE still exhibited the highest wear rate, and the wear rates of d-BP/PTFE composites were always lower than that of BP/PTFE. Apparently, the addition of BP and d-BP increased the tribological properties of the composites, and the reason why the content of d-BP was 5 wt.% showed the

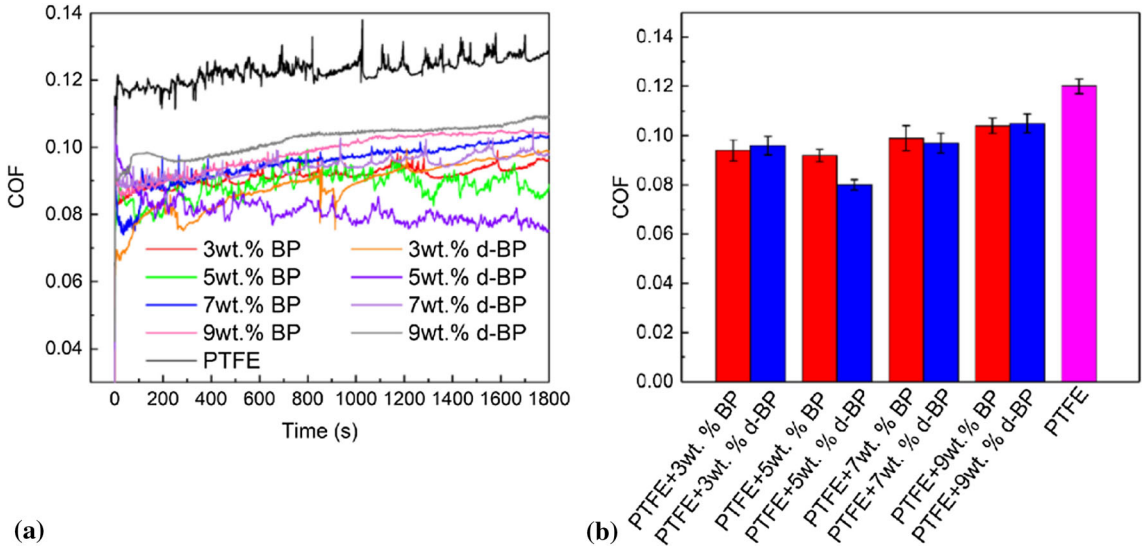

Fig. 4 (a) Variation curves in COFs as a function of time for pure PTFE- and PTFE-based composites with different BP and d-BP contents; (b) the average COFs of pure PTFE and the composites

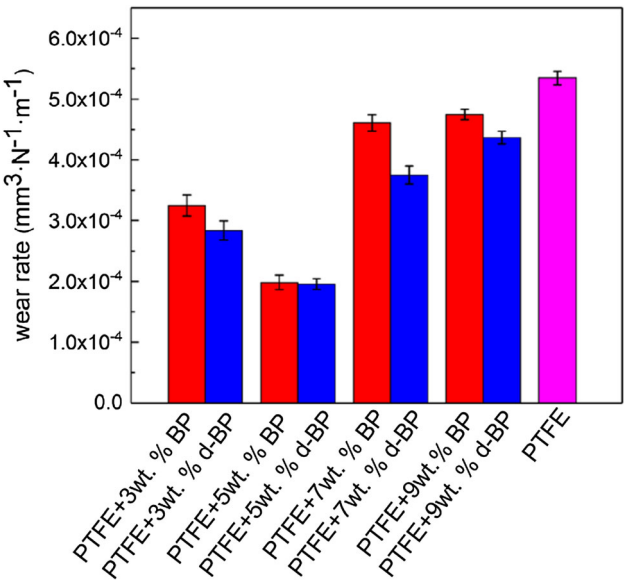

Fig. 5 Average wear rates of pure PTFE and the composites

best result can be concluded as the follows: When with a low content of fillers (3%), BP in the composite was totally oxidized and almost no surplus, resulting in BP was unable to exert its lubricating effect. And when the contents were high (7 and 9%), BP was not sufficiently oxidized, many powders still existed in the composites and aggregated, thus the corresponding COF were high. Herein, it is apparent that the composites both exhibit excellent tribological properties with the filler content of 5 wt.%. Thus, the composites with 5 wt.% d-BP and BP addition and the pure PTFE were chosen for further discussion.

3.1.1 Morphology of the Transfer Film. PTFE is easy to form a transfer film on the surface of the friction pairs during the friction process (Ref 42). Therefore, it is important to evaluate the transfer film. A digital microscope (VHX-6000, Keyence) was used to observe the transfer films on the counterpart balls. Obviously, each ball has a transfer film on the surface, and there is wear debris on the surface of counterpart balls. Apparently, the transfer film formed on the counterpart ball for the case of pure PTFE is not successive in Fig. 6a, indicating the poor wear resistance of PTFE. Besides, it can be easily speculated that the major component of the transfer film is PTFE, because nothing else was introduced during the friction process between the Si_3N_4 ball and the pure PTFE. As for the transfer film formed for the BP/PTFE and d-BP/PTFE composites, it is difficult to define the main components. Figure 7 exhibits the SEM and EDX results of the counterpart balls against with the BP/PTFE composite. The main element of the wear debris is F, indicating that the PTFE was peeled from the matrix and adhered on the surface of the ball, forming the wear debris. Meanwhile, the transfer film was mainly consisted of O and P. It can be speculated that the transfer film was formed by the oxidized BP. The result of the EDX patterns shows that the phosphorus oxides formed by the oxidation of BP played an important role in improving the wear resistance properties. Figure 8 shows the SEM and EDX results of the counterpart ball against the composites with 5 wt.% d-BP addition. Similar to the results shown in Fig. 7, PTFE was still the main part of wear debris, while the transfer film was mainly phosphorus oxides. Compared with the observed counterpart ball against PTFE, both the composites with BP and d-BP formed the steady, thin and smooth transfer films on the surfaces of the counterpart balls. The results exhibited that during the friction process, BP nanoflakes and d-BP nanoflakes were separated from the composites and formed a P_xO_y transfer film. The PTFE adhered on the surface of counterpart ball was pushed apart to form wear debris.

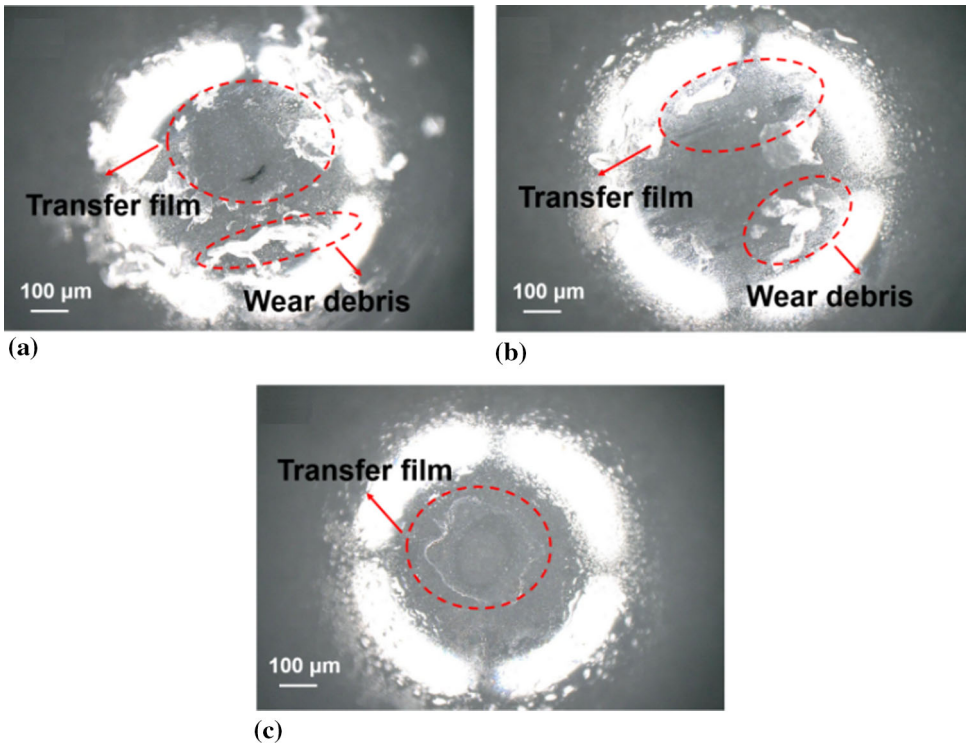

Fig. 6 SEM images of the counterpart balls: (a) PTFE; (b) 5 wt.% BP/PTFE; (c) 5 wt.% d-BP/PTFE

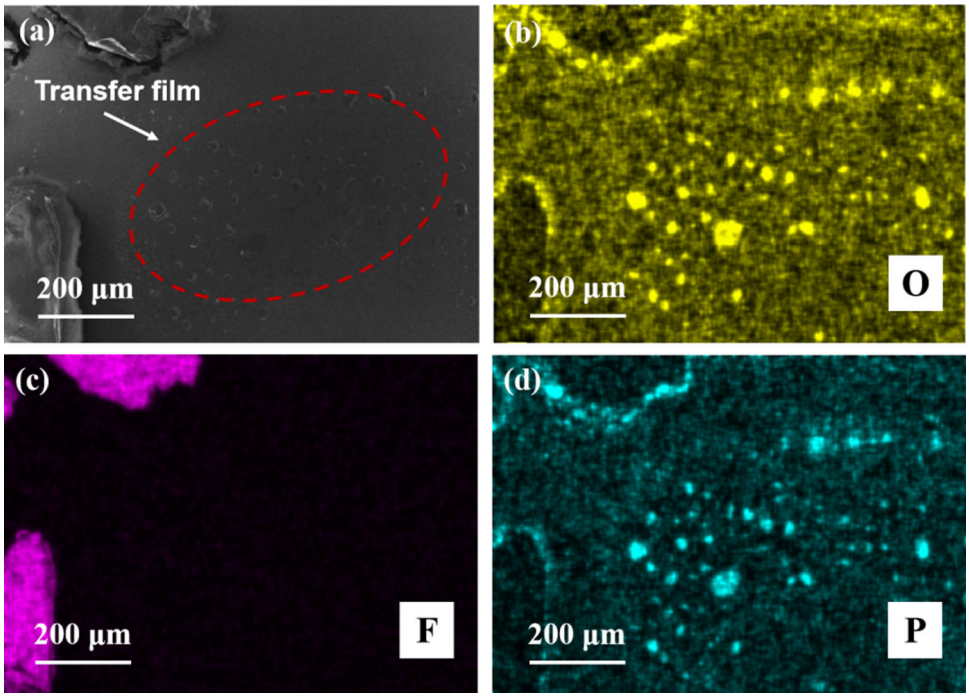

Fig. 7 (a) SEM image of the counterpart ball against 5 wt.% BP/PTFE; (b)-(d) are the element distribution images of oxygen, fluorine and phosphorus on the surface of the ball, respectively

3.1.2 Morphology of the Surface. In order to further explore the influence of the transfer film on the lubrication mechanism, SEM and EDX were carried out to analyze the worn surfaces on the composites. Figure 9 exhibits the morphology and the element distribution of the worn area on the BP/PTFE composite with 5 wt.% BP addition. It is obvious that typical flaky adhesion spalling pits and furrows along the sliding direction are the major surface characteristics. Compared with the element distribution images of F and P, BP was the main reason of the spalling pits. During the friction process, BP was subjected to shear forces and fell off from the surface and adhered on the surface of the counterpart ball. Meanwhile,

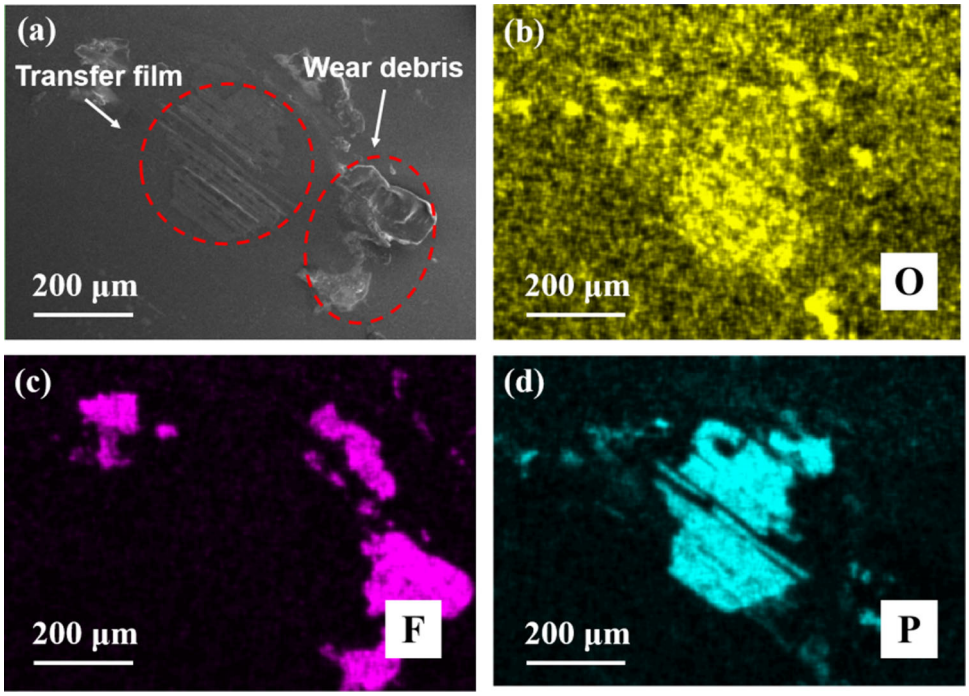

Fig. 8 (a) SEM image of the counterpart ball against 5 wt.% d-BP/PTFE; (b)-(d) are the element distribution images of oxygen, fluorine and phosphorus on the surface of the ball, respectively

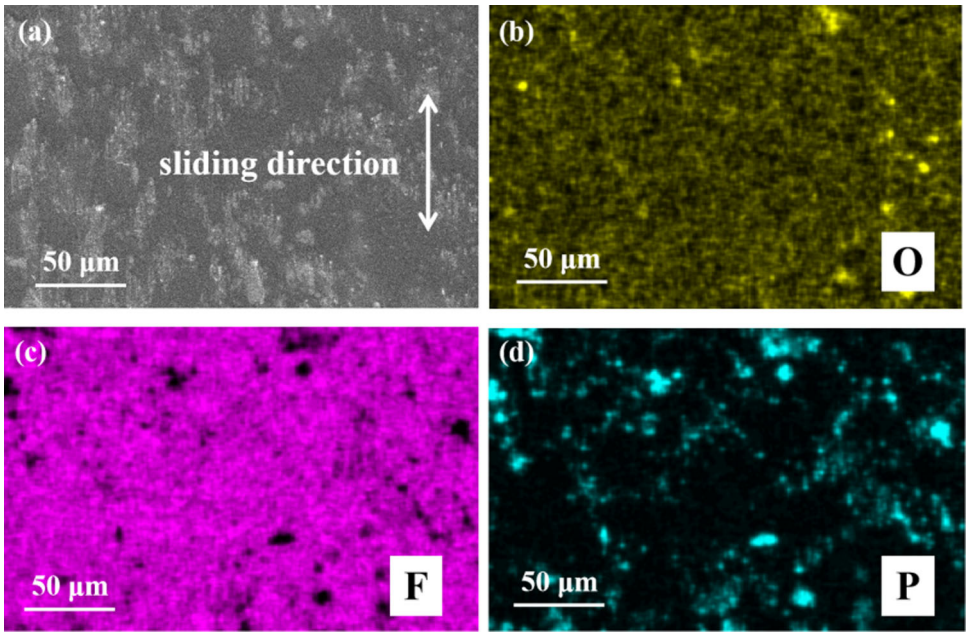

Fig. 9 (a) SEM image of the worn surface on the 5 wt.% BP/PTFE; (b)-(d) are the element distribution images of oxygen, fluorine and phosphorus of the surface, respectively

there is less O on the surface, exhibiting a small fraction of P was oxidized. The surface and the element distribution images of the worn area on the 5 wt.% d-BP/PTFE composite is shown in Fig. 10. Compared with the surface of 5 wt.% BP/PTFE, the number of spalling pits was significantly reduced, and the edge of the spalling pits were approximately perpendicular to the sliding direction. From the element distribution images, it can be seen that P still appeared at the position of the spalling pits, but the content of P in the observed region decreased. However, it is obvious that the content of O increased, and O is basically in the same place as P, proving that most of the P was oxidized, being consistent with the results of the actively control of BP oxidation. In order to further investigate the binding form of the elements on the worn surface, XPS was carried out to characterize the worn surface of the composites. The core-level spectra of P 2p and O 1s on the two kinds of composites

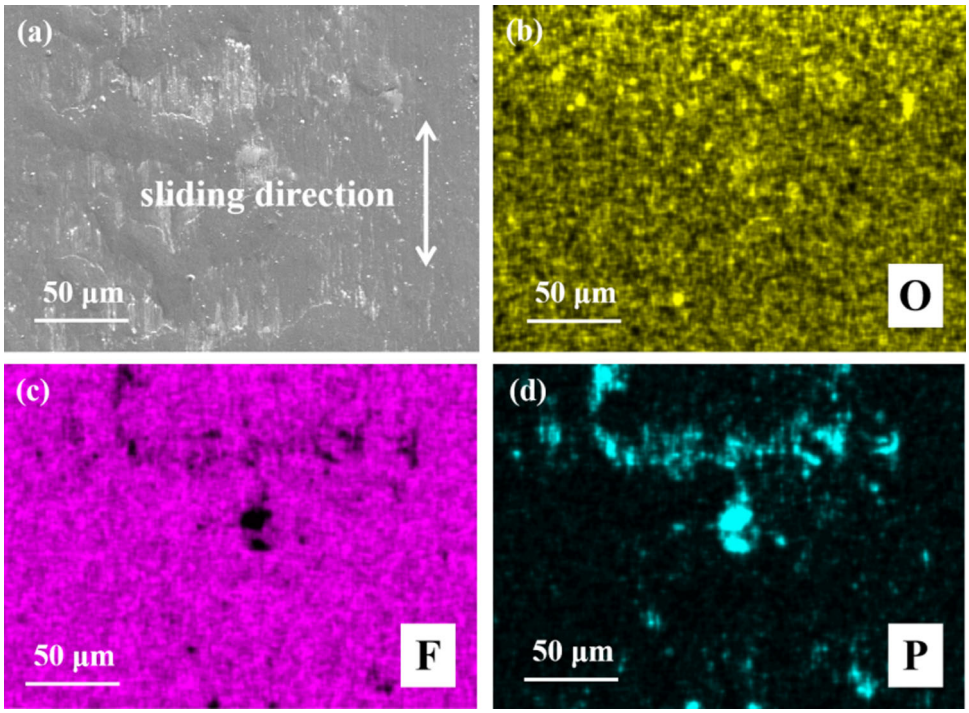

Fig. 10 (a) SEM image of the worn surface on the 5 wt.% d-BP/PTFE; (b)-(d) are the element distribution images of oxygen, fluorine and phosphorus of the surface, respectively

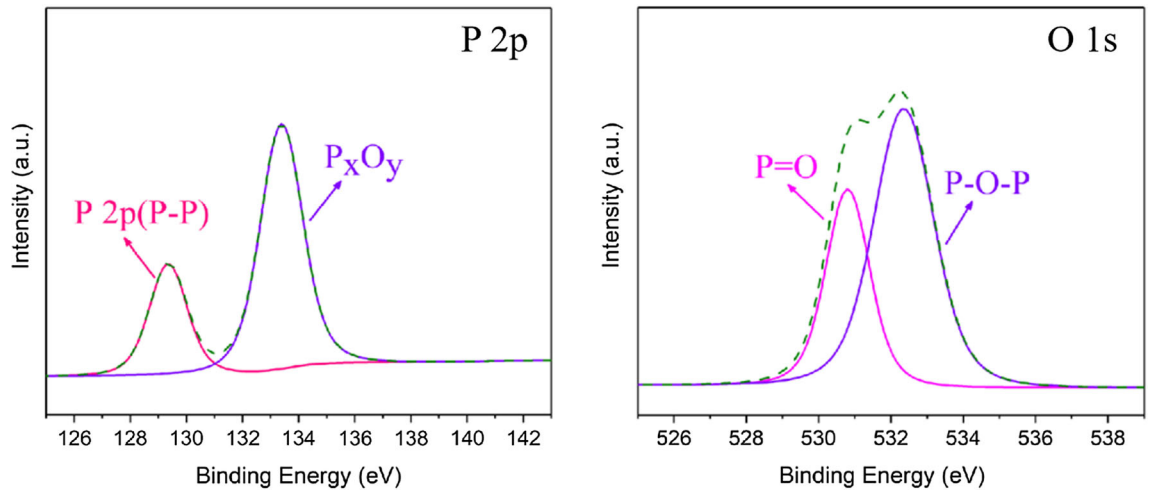

Fig. 11 X-ray photoelectron spectra of the elements on the worn surface of 5 wt. % BP/PTFE; (a)P2p; (b) O1s

are shown in Fig. 11 and 12, respectively. As shown in Fig 12(a), the peak at 129.3 eV corresponds to the P-P bonds of black phosphorus (Ref 43), while the peak in the range of 132-136 eV corresponds to the phosphorus oxide (Ref 44). Figure 11(b) shows the spectra of O 1s, and the peak at 530.9 and 532.2 eV represent the P=O bond and the P-O-P bond, respectively. The appearance of P=O bond and P-O-P bond further proved the oxidization of BP, owing to the easily oxidation character. On the basis of these results, it can be inferred that during the friction process, BP on the surface of the BP/PTFE composite was oxidized to P_xO_y for the formation of a lubricant film. With the constant relative movement of the counterpart ball and the composite, P_xO_y absorbed moisture from the air and then adhered on the surface of the ball, forming a transfer film on it. The direct contact of PTFE and the ball was converted to the contact of PTFE and the P_xO_y film. Meanwhile, the film protected PTFE from constantly transferring to the surface of the counterpart ball, and thus the COF and wear rate decreased. Figure 12 exhibits the XPS results of P 2p and O 1s on the worn surface of 5 wt.% d-BP/PTFE. Compared with the spectra of P 2p shown in Fig. 12 (a), the characteristic peak intensity of P-P in the spectrum of P 2p decreases. It was mainly due to the actively controlled oxidation of BP nanoflakes and this phenomenon was also confirmed by the peaks of O-P=O and P_2O_5. The peaks of O 1s in Fig. 13(b) also proved that a large amount of BP in 5 wt.% d-BP/PTFE was

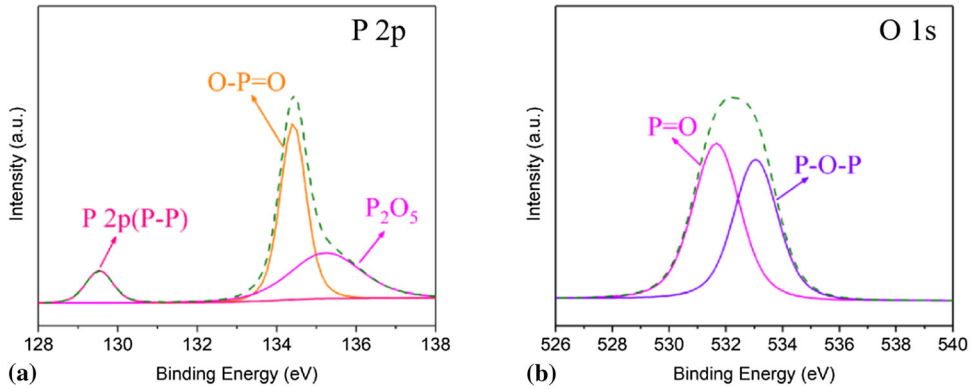

Fig. 12 X-ray photoelectron spectra of the elements on the worn surface of 5 wt.% d-BP/PTFE; (a) P2p; (b) O1s

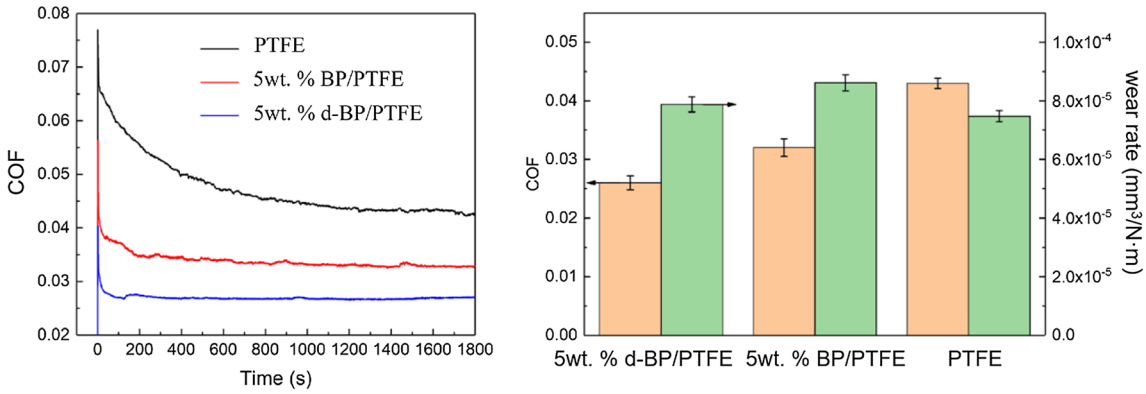

Fig. 13 (a) Variation curves in COFs as a function of time for pure PTFE and PTFE-based composites with 5 wt.% BP and d-BP under water-lubricated conditions; (b) the average COFs and the wear rates of pure PTFE and the composites under water-lubricated conditions

oxidized to P_xO_y, and the results exhibited that only a small amount of BP remained in the worn area. Due to the active oxidation of BP, more P_xO_y was present in the friction region, and thus the transfer film formed on the counterpart ball against 5 wt.% d-BP/PTFE was more continuous and compact. The transfer film led to the low COF of 5 wt.% d-BP/PTFE.

3.2 Tribological Tests Under Water-Lubricated Conditions

In consideration of the fact that the P_xO_y is easy to absorb moisture in the air, the tests under water-lubricated conditions were designed to further study the tribological performances of BP/PTFE and d-BP/PTFE composites. Because of the good lubrication performance of the composites with 5 wt.% of BP and d-BP under dry conditions, they were selected for the tribological experiments under water-lubricated conditions. The pure PTFE was also tested as the control experiment. As shown in Fig. 13(a), the COF values of the composites under water-lubricated conditions can be stabilized after about 200 s and then kept stable for a long time. The COF of the composite with 5 wt.% d-BP addition can even reduce to about 0.03. The average COFs of the three composites can be arranged as follows: PTFE (0.043) > 5 wt.% BP/PTFE (0.033) > 5 wt.% d-BP/PTFE (0.026), what should be noticed is that the COF of 5 wt.% d-BP/PTFE was reduced by 39.5% when compared with pure PTFE. The COF results indicated that the composites still had excellent lubrication performance when they were used in water environment. However, the results of the wear rates showed different trends: the 5 wt.% BP/PTFE had the highest wear rate, the 5 wt.% d-BP/PTFE composite intermediate, and PTFE the lowest wear rate. The reason can be explained as follows: During the friction process, BP and d-BP played the role to reduce friction. However, BP was unstable in water and oxygen phenomenon, it was easy to be oxidized to P_xO_y, which had a strong affinity for water and could be transformed to phosphoric acid. The resulting phosphoric acid would be carried away owing to the relative movement of the water. These reactions led to the reduction of the BP content in the materials, and thus, the wear was further aggravated as compared with the PTFE in the composites under water-lubricated conditions. In order to further explore the wear mechanism under water-lubricated conditions, SEM and XPS were used to characterize the counterpart balls and the worn surfaces. As shown in Fig. 14, the transfer film was very shallow and even hardly to be observed in the SEM image. However, the generation of P and O revealed that there was a thin film on the surface of the counterpart ball. The same case also appeared on the surface of the counterpart ball against the d-BP/PTFE composite. Figure 15 shows the SEM image and the corresponding element distribution. It can be seen that the transfer film is also very shallow, and P and O concentrate on the surface as the main components of the transfer film. The topography of the worn area of the 5 wt.% BP/PTFE after the tribological tests under water-lubricated conditions is shown in Fig. 16a. Significant exfoliation can be observed on the surface, proving that the main wear form was adhesive wear. In addition, the P and O elements on the surface reduced as compared with those after dry-friction tests. The phenomenon

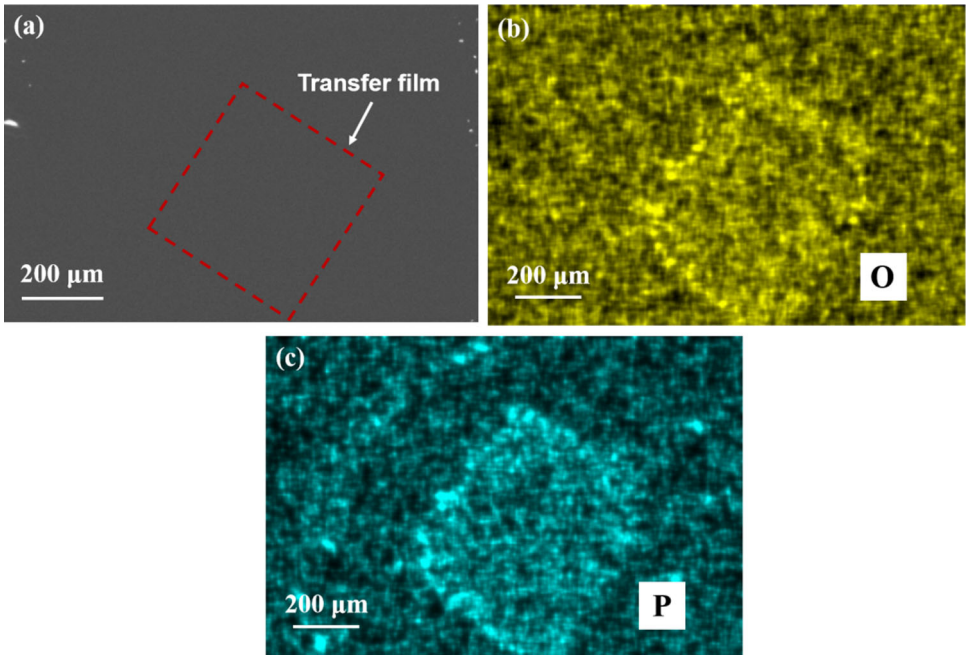

Fig. 14 (a) SEM image of the counterpart ball against 5 wt.% BP/PTFE after the tribological tests under water-lubricated conditions; (b) and (c) are the element distribution images of oxygen and phosphorus on the ball

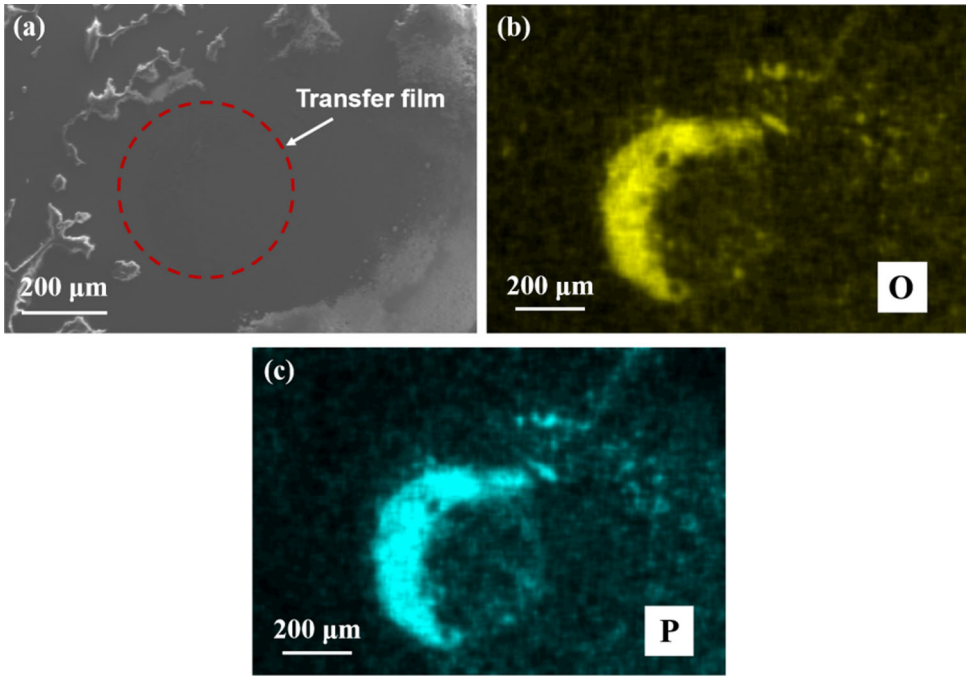

Fig. 15 (a) SEM image of the counterpart ball against 5 wt.% d-BP/PTFE after the tribological tests under water-lubricated conditions; (b), (c) are the element distribution images of oxygen and phosphorus on the ball surface

can be explained by the characteristics of BP that it is easy to be oxidized when exposed to oxygen and water. During the friction process, BP was oxidized to the P_xO_y, which was partly adhered on the surface of the counterpart ball, resulting in the exfoliation of the worn surface. Besides, part of the P_xO_y converted into phosphoric acid owing to the strong water solubility of P_xO_y. Most of the phosphoric acid was carried away with the relative motion of water. Thus, the amount of BP in the composite was sharply reduced, resulting in the high wear rate. In the case of the worn surface on the d-BP/PTFE composite after the tribological tests under water-lubricated conditions, as shown in Fig. 17, although there is still exfoliation, the wear mark is shallower. Besides, with the actively controlled oxidation of the BP nanoflakes, the formed P_xO_y could protect the internal residual BP from being further oxidized (Ref 46). Therefore, less P element was observed on the surface. XPS was used to characterize the binding form of the elements on the worn surfaces. As shown in Fig. 18, the

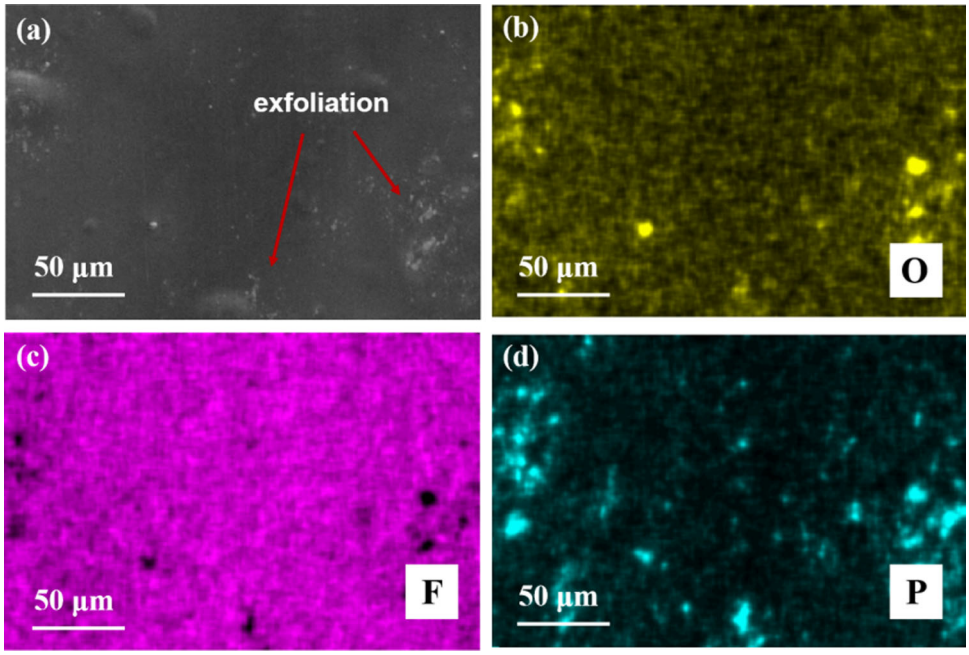

Fig. 16 (a) SEM image of the worn surface on the 5 wt.% BP/PTFE after the tribological tests under water-lubricated conditions; (b-d) are the element distribution images of oxygen, fluorine and phosphorus of the surface, respectively

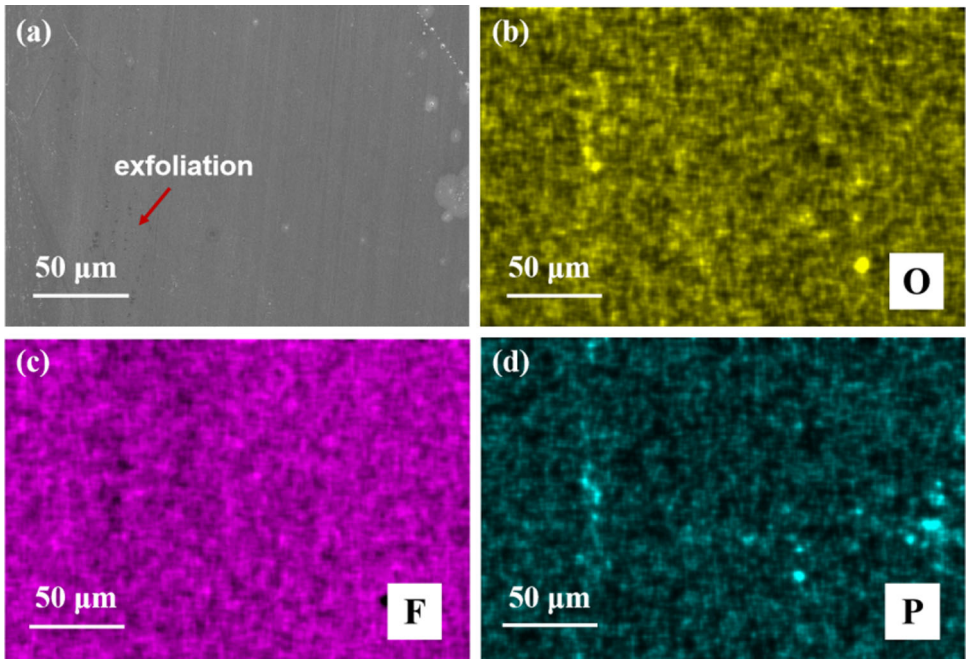

Fig. 17 (a) SEM image of the worn surface on the 5 wt.% d-BP/PTFE after the tribological tests under water-lubricated conditions; (b-d) are the element distribution images of oxygen, fluorine and phosphorus of the surface, respectively

oxidation of BP was more obvious in water environment, which can be verified by the new P_2O_5 peaks in the spectra of P 2p. Meanwhile, the peak intensity of P-P bond in Fig. 18c decreases sharply as compared with that in Fig. 18a, proving that most of the BP flakes has been oxidized. A new peak representing P-OH also appears in the spectra of O 1s. The hydrogen in the hydroxyl group can form hydrogen bonds with O in the water molecules, and hence, the hydroxyl groups in the phosphorus oxide on the surfaces of the composite and the counterpart ball could form a strongly adsorbed water layer at the friction interface, protecting the surface from direct dry-contact (Ref 45). Therefore, the COF of the composites had a sharp decrease in the water environment. On account of the actively controlled oxidation of BP, more hydroxyl groups existed on the surface of the d-BP/PTFE composite, giving rise to the lower COF than the BP/PTFE composite.

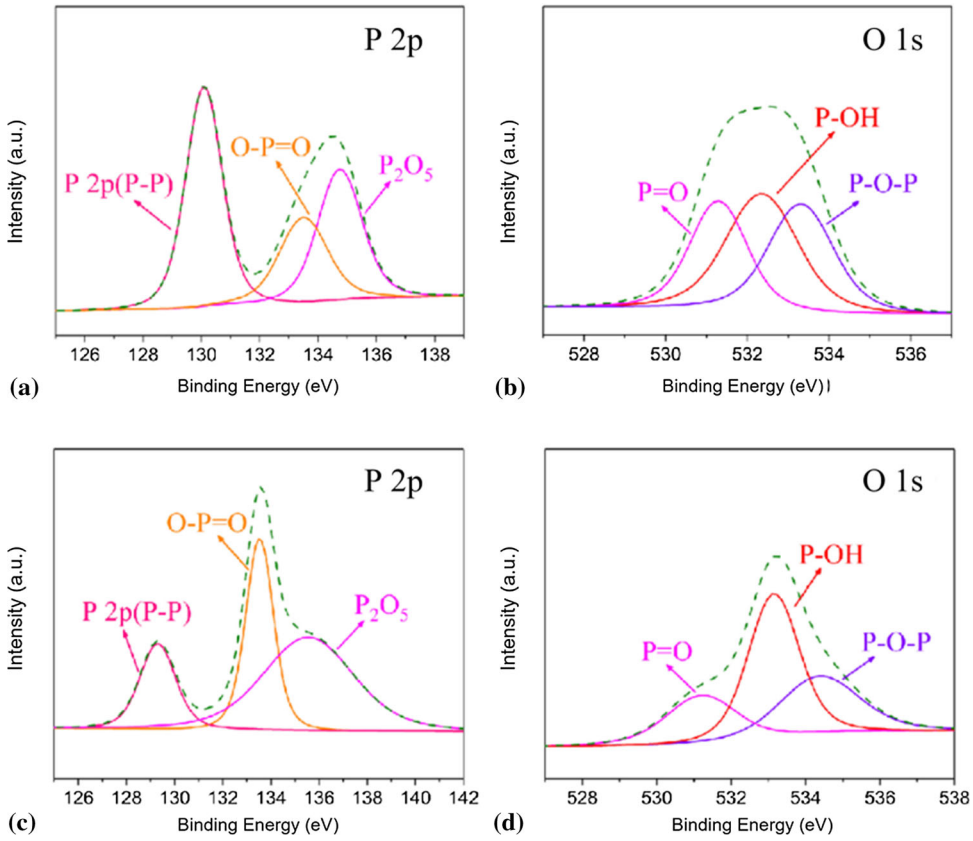

Fig. 18 X-ray photoelectron spectra of the elements on the worn surface of the composites after the tribological tests under water-lubricated conditions; (a) and (b) are P2p and O1s on the surface of 5 wt.% BP/PTFE composite, respectively; (c) and (d) are P2p and O1s on the surface of 5 wt.% d-BP/PTFE composite, respectively

4. Conclusions

The tribological behaviors of the BP/PTFE and d-BP/PTFE composites as well as pure PTFE against Si_3N_4 balls were investigated under dry-friction and water-lubricated conditions, and the underlying lubrication mechanisms were explored. The conclusions are summarized as follows

1) As compared with the pure PTFE, the BP/PTFE and d-BP/PTFE composites exhibited excellent lubrication properties. When the content of BP or d-BP was 5 the composites corresponded to the optimal tribological properties. For the experiments under dry-friction conditions, as compared with the pure PTFE, the COF were reduced by 23.3 and 35% for the composites with 5 wt.% BP and 5 wt.% d-BP, respectively, and the wear rates were reduced by 62.9 and 63.4%.
2) Under the dry-friction conditions, the oxidation of BP caused the low COF of the composites, and the P_xO_y produced by BP oxidation could form a lubricating transfer film, which can reduce the COF and wear rate.
3) For the experiments under water-lubricated conditions, the COF can be reduced by 39.5% for the composite with 5 wt.% d-BP. Although the 5 wt.% d-BP/PTFE has a slightly higher wear rate than pure PTFE, it showed the best comprehensive tribological properties among all the composites investigated in this work.
4) The P-OH bonds on the surfaces of composites could absorb water molecules when they were in the water environment, forming an adsorbed water layer at the friction interface, giving rise to the reduction of the COF.
5) All the above work has demonstrated that adding d-BP can bring a positive effect in the tribological properties of PTFE, and the further experiment illustrated that the composites can play a better role in water. This has given us an inspiration about using such composites as engineering material, especially in fabricating some essential parts of equipment work under water.

Acknowledgments

This work was supported by the National Natural Science Foundation of China (Grant No. 51822505) and the Pre-Research Program in National 14th Five-Year Plan (Grant No. 80923010602).

References

1. S.H. Sohn, T.H. Kim, T.S. Kim, T.J. Min, J.H. Lee, S.M. Yoo, J.W. Kim, J.E. Lee, C.H. Kim, S.H. Park, and W.M. Jo, Evaluation of 3D Templated Synthetic Vascular Graft Compared with Standard Graft in a Rat Model: Potential use as an Artificial Vascular Graft in Cardiovascular Disease, *Mat*, 2021, **14**(5), p 1239. https://doi.org/10.3390/ma14051239

2. M.U.A. Khan, R. Raad, F. Tubbal, P.I. Theoharis, S.N. Liu, and J. Foroughi, Bending Analysis of Polymer-Based Flexible Antennas for Wearable, General IoT Applications: A Review, *Polym*, 2021, **13**(3), p 357. https://doi.org/10.3390/polym13030357
3. I. Valiente-Blanco, J.L. Perez-Diaz, J.L. Perez-del-Alamo, and E. Diez-Jimenez, Temperature Dependence of the Friction Coefficient of Grease-Lubricated PTFE Linear Bushings Against Titanium Grade 5 Alloy (Ti6Al4V) and Life Tests Operating at High-Speed, *J. Tribol-Trans. Asme.*, 2020, **142**(9), 091701. https://doi.org/10.1115/1.4046708
4. J.Y. Lee, and D.S. Lim, Tribological behavior of PTFE Film with Nanodiamond, *Surf. Coat. Technol.*, 2004, **188**, p 534–538. https://doi.org/10.1016/j.surfcoat.2004.07.102
5. Y.Q. Gu, Z.D. Wang, S.G. Peng, T.B. Ma, and J.B. Luo, Quantitative Measurement of Transfer Film Thickness of PTFE Based Composites by Infrared Spectroscopy, *Tribol. Int.*, 2021, **153**, 106593. https://doi.org/10.1016/j.triboint.2020.106593
6. L. Ding, D. Axinte, P. Butler-Smith, and A.A. Hassan, Study on the Characterisation of the PTFE Transfer Film and the Dimensional Designing of Surface Texturing in a Dry-Lubricated Bearing System, *Wear*, 2020, **448**, 203238. https://doi.org/10.1016/j.wear.2020.203238
7. H. Unal, A. Mimaroglu, U. Kadioglu, and H. Ekiz, Sliding Friction and Wear Behaviour of Polytetrafluoroethylene and Its Composites Under Dry Conditions, *Mater. Des.*, 2004, **25**(3), p 239–245. https://doi.org/10.1016/j.matdes.2003.10.009
8. T.A. Blanchet, and Y.L. Peng, Wear resistant irradiated FEP unirradiated PTFE composites, *Wear*, 1998, **214**(2), p 186–191. https://doi.org/10.1016/S0043-1648(97)00254-8
9. M.S. Park, H.S. Sung, C.H. Park, T.S. Han, and J.H. Kim, High Tribology Performance of Poly(Vinylidene Fluoride) Composites Based on Three-Dimensional Mesoporous Magnesium Oxide Nanosheets, *Comp. Part B-Eng.*, 2019, **163**, p 224–235. https://doi.org/10.1016/j.compositesb.2018.10.096
10. G. Suresh, V. Vasu, and M.V. Rao, A Composite (Taguchi-Utility-RSM) Approach for Optimizing the Tribological Responses of Polytetrafluoroethylene (PTFE) Nanocomposites for Self-lubrication Applications, *SILICON*, 2018, **10**(5), p 2043–2053. https://doi.org/10.1007/s12633-017-9718-7
11. O.V. Gogoleva, A.A. Okhlopkova, and P.N. Petrova, Development of Self-Lubricating Antifriction Materials Based on Polytetrafluoroethylene and Modified Zeolites, *J. Frict. W.*, 2014, **355**(5), p 383–388. https://doi.org/10.3103/S1068366614050055
12. Z.N. Jia, and Y.L. Yang, Effects of LaF3/CeF3 on the Friction Transfer of PTFE-Based Composites, *Tribol. Int.*, 2021, **161**, 107069. https://doi.org/10.1016/j.triboint.2021.107069
13. D.P. Gu, S.Y. Liu, S.W. Chen, K.F. Song, B.C. Yang, and D. Pan, Tribological Performance of Si3N4-PTFE Composites Prepared by High-Pressure Compression Molding, *Tribol. Trans.*, 2020, **63**(4), p 756–769. https://doi.org/10.1080/10402004.2020.1742407
14. A.Y. Wang, B. Lin, H.B. Zou, C.B. Wei, Y.Q. Meng, T.Y. Sui, and S. Yan, Effect of Micrometer Sized Ceramic Particles on the Tribological Properties of Polytetrafluoroethylene Based Composites, *Surf. Topogr-Metro. Propert.*, 2020, **8**(3), 035005. https://doi.org/10.1088/2051-672X/aba485
15. X. Teng, L.F. Wen, Y.X. Lv, W.G. Tang, X.G. Zhao, and C.H. Chen, Effects of Potassium Titanate Whisker and Glass Fiber on Tribological and Mechanical Properties of PTFE/PEEK Blend, *High. Perform. Polym.*, 2018, **30**(6), p 752–764. https://doi.org/10.1177/0954008317723444
16. Y.Y. Liu, N. Xu, Y. Wang, Y.T. Yao, H.Y. Xiao, J. Jia, H.B. Lv, and D.X. Zhang, Preparation and Tribological Properties of Hybrid PTFE/Kevlar Fabric Self-Lubricating Composites, *Surf. Coat. Technol.*, 2019, **361**, p 196–205. https://doi.org/10.1016/j.surfcoat.2018.12.121
17. F.Z. Song, Z.H. Yang, G. Zhao, Q.H. Wang, X.R. Zhang, and T.M. Wang, Tribological Performance of Filled PTFE-Based friction material for Ultrasonic Motor Under Different Temperature and Vacuum Degrees, *J. Appl. Polym. Sci.*, 2017, **134**(39), p 45358. https://doi.org/10.1002/app.45358
18. L. Zhang, G.X. Xie, S. Wu, S.G. Peng, X.Q. Zhang, D. Guo, S.Z. Wen, and J.B. Luo, Ultralow Friction Polymer Composites Incorporated with Monodispersed Oil Microcapsules, *Friction*, 2021, **9**(1), p 29–40. https://doi.org/10.1007/s40544-019-0312-4
19. G. Gao, J. Gong, Y. Qi, J.F. Ren, H.G. Wang, D.Y. Yang, and S.S. Chen, Tribological Behavior of PTFE Composites Filled with PEEK and Nano-ZrO2, *Tribol. Trans.*, 2020, **63**(2), p 296–304. https://doi.org/10.1080/10402004.2019.1687796
20. P. Zhao, J.Z. Liu, Q.H. Wang, L.J. Yang, and X.L. Li, Study on the Tribological Properties of Ekonol-PI-PTFE Composites, *J. Mater. Sci. Eng.*, 2003, **21**(6), p 851–854.
21. Z.Y. Chen, H.X. Yan, L.L. Guo, Y.B. Feng, L. Li, W.X. Feng, P.F. Yang, B. Liu, T.Y.F. Liu, and J.S. Yuan, Investigation of Mechanical and Frictional Performance for Bismaleimide Composites Reinforced by Hyperbranched Polysiloxane-Cyclophosphazene Functionalized Rgo/Mos2, *J. Alloy. Compd.*, 2020, **823**, 153837. https://doi.org/10.1016/j.jallcom.2020.153837
22. L.W. Mu, J.H. Zhu, J.D. Fan, Z.X. Zhou, Y.J. Shi, X. Feng, H.Y. Wang, and X.H. Lu, Self-Lubricating Polytetrafluoroethylene/Polyimide Blends Reinforced with Zinc Oxide Nanoparticles, *J. Nanomater.*, 2015, **2015**, 545307. https://doi.org/10.1155/2015/545307
23. S. Zhang, T.B. Ma, A. Erdemir, and Q.Y. Li, Tribology of Two-Dimensional Materials, From Mechanisms to Modulating Strategies, *Mater. Today*, 2019, **26**, p 67–86. https://doi.org/10.1016/j.mattod.2018.12.002
24. X.L. Wang, B.X. Liu, G.H. Zhang, L.W. Liu, Q. Chen, W.J. Chen, and X.Y. Li, Effect of Atomic Oxygen Irradiation on the Structural and Tribological Characteristics of Polytetrafluoroethylene and its Composites, *Surf. Interface .Anal.*, 2017, **49**(2), p 112–116. https://doi.org/10.1002/sia.6066
25. Z.B. Sun, H.H. Xie, S.Y. Tang, X.F. Yu, Z.N. Guo, J.D. Shao, H. Zhang, H. Huang, H.Y. Wang, and P.K. Chu, Ultrasmall Black Phosphorus Quantum Dots, Synthesis and use as Photothermal Agents, *Angewandte. Chemie-Int. Edit.*, 2015, **54**(39), p 11526–11530. https://doi.org/10.1002/anie.201506154
26. Y.Q. Wang, X.X. Hu, L.L. Zhang, C.L. Zhu, J. Wang, Y.X. Li, Y.L. Wang, C. Wang, Y.F. Zhang, and Q. Yuan, Bioinspired Extracellular Vesicles Embedded With Black Phosphorus for Molecular Recognition-Guided Biomineralization, *Nat. Commun.*, 2019, **10**, p 2829. https://doi.org/10.1038/s41467-019-10761-5
27. P.V. Hlophe, and L.N. Dlamini, Synthesis of a Semi-Conductor-like MOF with Black Phosphorous as a Composite for Visible Light-Driven Photocatalysis, *RSC. Adv.*, 2019, **9**(64), p 37321–37330. https://doi.org/10.1039/c9ra08296d
28. M. Galluzzi, Y.L. Zhang, and X.F. Yu, Mechanical Properties and Applications of 2D Black Phosphorus, *J. Appl. Phys.*, 2020, **128**(23), 230903. https://doi.org/10.1063/5.0034893
29. W. Wang, G.X. Xie, and J.B. Luo, Black Phosphorus as a New Lubricant, *Frict*, 2018, **6**(1), p 116–142. https://doi.org/10.1007/s40544-018-0204-z
30. Q.J. Wang, T.L. Hou, W. Wang, G.L. Zhang, Y. Gao, and K.S. Wang, Tribological Behavior of Black Phosphorus Nanosheets as Water-Based Lubrication Additives, *Frict*, 2021 https://doi.org/10.1007/s40544-020-0465-1
31. Q.J. Wang, T.L. Hou, W. Wang, G.L. Zhang, Y. Gao, and K.S. Wang, Tribological Properties of Black Phosphorus Nanosheets as Oil-Based Lubricant Additives for Titanium Alloy-Steel Contacts, *R. Soc. Open. Sci.*, 2020, **7**(9), 200530. https://doi.org/10.1098/rsos.200530
32. G. Tang, F. Su, X. Xu, and P.K. Chu, 2D Black Phosphorus Dotted with Silver Nanoparticles, An Excellent Lubricant Additive for Tribological Applications, *Chem. Eng. J.*, 2020, **392**, p 123631. https://doi.org/10.1016/j.cej.2019.123631
33. S.G. Peng, Y. Guo, G.X. Xie, and J.B. Luo, Tribological behavior of Polytetrafluoroethylene Coating Reinforced with Black Phosphorus Nanoparticles, *Appl. Surf. Sci.*, 2018, **441**, p 670–677. https://doi.org/10.1016/j.apsusc.2018.02.084
34. Y. Lv, W. Wang, G. Xie, and J. Luo, Self-Lubricating PTFE-Based Composites with Black Phosphorus Nanosheets, *Tribol. Lett.*, 2018, **66**(2), p 61. https://doi.org/10.1007/s11249-018-1010-5
35. D. Hanlon, C. Backes, E. Doherty, C.S. Cucinotta, N.C. Berner, C. Boland, K. Lee, A. Harvey, P. Lynch, and Z. Gholamvand, Liquid Exfoliation of Solvent-Stabilized Few-Layer Black Phosphorus for Applications Beyond Electronics, *Nat. Commun.*, 2015, **6**, p 8563. https://doi.org/10.1038/ncomms9563
36. S. Walia, S. Balendhran, T. Ahmed, M. Singh, C. El-Badawi, M.D. Brennan, P. Weerathunge, M.N. Karim, F. Rahman, and A. Rassell, Ambient Protection of Few-Layer Black Phosphorus via Sequestration of Reactive Oxygen Species, *Adv. Mater.*, 2017, **29**(27), p 1700152. https://doi.org/10.1002/adma.201700152
37. X.Y. Ren, X. Yang, G. Xie, F. He, R. Wang, C. Zhang, D. Guo, and J. Luo, Superlubricity Under Ultrahigh Contact Pressure Enabled by Partially Oxidized Black Phosphorus Nanosheets, *Npj 2D. Mater. Appl.*, 2021, **5**(1), p 44. https://doi.org/10.1038/s41699-021-00225-0

38. S. Wu, F. He, G.X. Xie, Z.L. Bian, Y.L. Ren, X.Y. Liu, H.J. Yang, D. Guo, L. Zhang, and S.Z. Wen, Super-Slippery Degraded Black Phosphorus/Silicon Dioxide Interface, *ACS. Appl. Mater. Interfaces.*, 2020, **12**(6), p 7717–7726. https://doi.org/10.1021/acsami.9b19570
39. S. Wu, F. He, G.X. Xie, Z.L. Bian, J.B. Luo, and S.Z. Wen, Black Phosphorus, Degradation Favors Lubrication, *Nano. Lett.*, 2018, **18**(9), p 5618–5627. https://doi.org/10.1021/acs.nanolett.8b02092
40. F.T. Johra, and W.G. Jung, Synthesis of Black Phosphorus via a Facile Vapor Transfer Method, *Electron. Mater. Lett.*, 2019, **15**(5), p 639–644. https://doi.org/10.1007/s13391-019-00162-7
41. A.L. Greer, K.L. Rutherford, and M. Hutchings, Wear Resistance of Amorphous Alloys and Related Materials, *Int. Mater. Rev.*, 2002, **47**(2), p 87–112. https://doi.org/10.1179/095066001225001067
42. N.L. McCook, D.L. Burris, G.R. Bourne, J. Steffens, J.R. Hanrahan, and W.G. Sawyer, Wear Resistant Solid Lubricant Coating Made from PTFE and Epoxy, *Tribol. Lett.*, 2005, **18**(1), p 119–124. https://doi.org/10.1007/s11249-004-1766-7
43. M.T. Edmonds, A. Tadich, A. Carvalho, A. Ziletti, K.M. O'Donnell, S.P. Koenig, D.F. Coker, B. Ozyilmaz, A.H.C. Neto, and M.S. Fuhrer, Creating a Stable Oxide at the Surface of Black Phosphorus, *ACS Appl. Mater. Interfaces.*, 2016, **7**(27), p 14557–14562. https://doi.org/10.1021/acsami.5b01297
44. K.L. Kuntz, R.A. Wells, J. Hu, T. Yang, B.J. Dong, H.H. Guo, A.H. Woomer, D.L. Druffel, A. Alabanza, and D. Tomanek, Control of Surface and Edge Oxidation on Phosphorene, *ACS. Appl. Mater. Interfaces.*, 2017, **9**(10), p 9126–9135. https://doi.org/10.1021/acsami.6b16111
45. X.Y. Ren, X. Yang, G.X. Xie, and J.B. Luo, Black Phosphorus Quantum Dots in Aqueous Ethylene Glycol for Macroscale Superlubricity, *Acs. Applied. Nano. Materials.*, 2020, **3**(5), p 4799–4809. https://doi.org/10.1021/acsanm.0c00841
46. H.Y. Nan, X.Y. Wang, J. Jiang, K. Ostrikov, Z.H. Ni, X.F. Gu, and S.Q. Xiao, Effect of the Surface Oxide Layer on the Stability of Black Phosphorus, *Appl. Surf. Sci.*, 2021, **537**, 147850. https://doi.org/10.1016/j.apsusc.2020.147850